


Elastic Modulus and Hardness of Potassium Tantalum Germanate Glasses and Glass-Ceramics

Clarissa L. Justino de Lima^{a,b,*} , Fred A. Veer^c, Branko Šavija^b, Fabia Castro Cassanjes^d,
Gael Y. Poirier^d

^aAmerican Glass Research, Delft, The Netherlands.

^bDelft University of Technology, Faculty of Civil Engineering and Geosciences, Delft, The Netherlands.

^cDelft University of Technology, Faculty of Architecture and the Built Environment, Delft, The Netherlands.

^dUniversidade Federal de Alfenas (UNIFAL), Instituto de Ciência e Tecnologia, Poços de Caldas, MG, Brasil.

Received: May 04, 2022; Revised: October 10, 2022; Accepted: October 14, 2022

Whilst the optical and structural properties of the glasses containing tantalum oxide have been considerably investigated, research into their mechanical properties is not substantially established. This work reports on the mechanical characterization of transparent germanate glass samples, obtained via the melt-quenching technique, with a molar content of Ta₂O₅ ranging from 0% to 20%. The introduction of Ta₂O₅ in the samples is related to significant improvements in the mechanical properties. The transition from glass to transparent glass-ceramic via the controlled crystallization of Ta₂O₅ proved to be a tool to increase both the elastic modulus and the hardness while keeping the transparency of the material. The average elastic modulus of the studied compositions ranged from 69.2 GPa to 99.1 GPa, while the average hardness of the same samples varied from 5.10 GPa to 7.34 GPa.

Keywords: Tantalum oxide, glass, germanium oxide, nanoindentation.

1. Introduction

The wide applications of glassy materials, from construction and electronics to covers of smartphones, are continuously demanding innovative and stronger glasses. Glasses with high elastic moduli and high hardness values have been required for many years because the thickness of sheet glass with these properties can be decreased while preserving its strength. Thinner and lighter glasses are in demand for windows in buildings and cars, substrates for thin-film transistor (TFT) displays, and covers of smartphone¹. Among other reasons, the development of these innovative glasses is possible in connection with the evolution of the understanding of the property response as a function of the chemical composition. Therefore, it is important to determine the quantitative relation of each constituent element and its contribution to the final properties of the glass².

The Makishima-Mackenzie (MM) model provides a direct calculation of the Young's modulus of oxide glasses from chemical compositions. The prediction is based on an assessment of the dissociation energy of the oxide constituents and the packing density³. The model relates the bulk stiffness to the strength of the bonds and their density. The strength of the bonds is estimated from the dissociation energy, while the bond density is related to the combination of specific bond energy and atomic packing fraction⁴. A paper from Yamane and Mackenzie⁵ provides evidence that the Vickers hardness of the glasses is directly related to their bond strengths and the elastic moduli. Consequently, the use of elements with large dissociation energies and high atomic packing fractions

could be a path to follow in order to produce glasses with high elastic moduli and hardness.

Transition metal oxides are well-known and largely used for incorporation in vitreous materials due to optical changes and property enhancements owing to the insertion of these metallic ions inside the vitreous network. Furthermore, transition metal oxides usually increase the chemical and thermal stabilities of glass formers due to their intermediary behavior related to the high coordination number of the metallic ions and resulting higher connectivities of the glass network⁶⁻⁹.

Tantalum oxide (Ta₂O₅) has been less investigated due its lower solubility in glass formers as well as harder synthesis conditions related to melting temperatures¹⁰. To our knowledge, research into the mechanical properties of glasses containing Ta₂O₅ has just recently started and study of the mechanical properties of germanate glasses containing Ta₂O₅ is new. In fact, recent works have shown that tantalum germanate glasses are promising optical materials for luminescent and optical non-linear devices, but such applications are strongly dependent on sufficient mechanical performance¹¹⁻¹³.

Tantalum oxide (Ta₂O₅) has a large dissociation energy ($G_{\text{Ta}_2\text{O}_5} = 95.6 \text{ kJ/cm}^3$) and large cationic field strength (Ta⁵⁺)¹. Based on the Makishima and Mackenzie model, it is expected that an increasing tantalum content would lead to increasing elastic modulus.

Germanium oxide (GeO₂) possesses dissociation energy (G_{GeO_2}) varying from 44.9 to 49.5 kJ/cm³¹⁴, depending on the oxygen coordination number, which can be 4 or 6. This value is not large in relation to the dissociation energy of other

*e-mail: cdelima@agrntl.com

oxides. For instance, $G_{\text{SiO}_2} = 68 \text{ kJ/cm}^3$, and $G_{\text{Al}_2\text{O}_3} = 131 \text{ kJ/cm}^3$.¹⁵ However, the melting point of GeO_2 is low in relation to the melting point of both of these oxides. A glass with high amounts of both SiO_2 and Ta_2O_5 , or both Al_2O_3 and Ta_2O_5 , would require very high melting temperatures and probably special preparation techniques, such as the aerodynamic levitation technique. This technique was used, for instance, to prepare a glass with the composition $54\text{Al}_2\text{O}_3\cdot 46\text{Ta}_2\text{O}_5$ at a temperature of $2000 \text{ }^\circ\text{C}$.¹ Besides enabling the melting at an elevated temperature, the use of aerodynamic levitation also prevented crystallization of this composition.

Ta-based bulk metallic glasses with high fracture strength (2.7 GPa, obtained from compressive tests), hardness (9.7 GPa), and elastic modulus (170 GPa) were already reported¹⁶. However, due to their glass transition temperatures, above $700 \text{ }^\circ\text{C}$, these samples were prepared by arc melting of pure Ta, Ni, and Co, followed by copper mold suction casting preparation of the alloy rods.

The use of special melting techniques would be significantly more expensive than the traditional melt-quenching method. Furthermore, it would limit the size of the samples obtained to millimeters in diameter, thereby limiting the potential of the production on an industrial scale. For these reasons, this work focuses on the preparation of the samples via the melt-quenching method, at a maximum temperature of $1450 \text{ }^\circ\text{C}$. A series of glasses were prepared with GeO_2 , K_2O and Ta_2O_5 as constituent elements. Samples with variable contents of GeO_2 and Ta_2O_5 were characterized in order to quantify the effect of such changes on the mechanical properties of the glasses. These samples were already reported on and had their optical properties described by De Pietro et. al.¹⁷.

Based on these considerations, this work investigates the effect of the addition of Tantalum Oxide (Ta_2O_5) on the mechanical properties of germanate glasses. One sample was submitted to a heat treatment in order to obtain a glass-ceramic and compare its properties with the properties of the parent glass.

2. Experimental Part

The samples in the ternary system $(90-x)\text{GeO}_2\cdot 10\text{K}_2\text{O}\cdot (x)\text{Ta}_2\text{O}_5$ were prepared from the chemical compounds GeO_2 ($\geq 99.99\%$), Ta_2O_5 (99.9%) and K_2CO_3 ($\geq 99\%$), all from Aldrich, and melted in a platinum crucible. The starting compounds were weighted with an analytical balance and ground with a ceramic mortar and pestle before being placed in a crucible and molten. Each sample weighed 30 g. Melting temperatures ranged between $1300 \text{ }^\circ\text{C}$ and $1450 \text{ }^\circ\text{C}$, the samples being melted in temperatures that were as low as possible. The furnace was heated at $5 \text{ }^\circ\text{C}/\text{min}$. The samples were kept at the melting temperature for 45 min. The melts were cooled in the crucible by removing it from the furnace and pouring it into a stainless-steel mould.

After having been cooled to room temperature the samples were annealed for 3 h at a temperature immediately below the glass transition temperature, before cooling down to room temperature. The sample subjected to a heat treatment for obtaining a glass-ceramic was heat-treated for 48 h at $840 \text{ }^\circ\text{C}$ by heating at $3.6 \text{ }^\circ\text{C}/\text{min}$. The surfaces of the glass samples were ground and polished. All the produced samples are listed in Table 1.

Table 1. Melting conditions and compositions in the system $(90-x)\text{GeO}_2\cdot 10\text{K}_2\text{O}\cdot (x)\text{Ta}_2\text{O}_5$, with x varying from 0 to 20% mol.

Sample (x)	Theoretical composition	Melting temperature ($^\circ\text{C}$)
0	$90\text{GeO}_2\cdot 10\text{K}_2\text{O}$	1300
5	$85\text{GeO}_2\cdot 10\text{K}_2\text{O}\cdot 5\text{Ta}_2\text{O}_5$	1300
10	$80\text{GeO}_2\cdot 10\text{K}_2\text{O}\cdot 10\text{Ta}_2\text{O}_5$	1350
15	$75\text{GeO}_2\cdot 10\text{K}_2\text{O}\cdot 15\text{Ta}_2\text{O}_5$	1400
20	$70\text{GeO}_2\cdot 10\text{K}_2\text{O}\cdot 20\text{Ta}_2\text{O}_5$	1450

The samples were subjected to nanoindentation tests, thermal analysis and Energy-Dispersive X-ray Spectroscopy. The nanoindentation tests were performed at 700 nm of depth, at least 15 indentations per sample, with a distance of 20 nm between them, using a Nano Indenter MTS G200. The elastic modulus and hardness were obtained from the Berkovich nanoindentation curve. The average values of both properties were calculated based on the load-displacement curves of the samples. The calculation of E using nanoindentation is not straightforward. A reduced Young's modulus, $E_r = E/(1-\nu^2)$, is obtained¹⁸, in which ν is the Poisson's ratio.

SEM-EDS and microscopy analysis were performed by a Philips XL30 ESEM machine. The calculations of both elastic modulus and hardness considered the penetration depth between 300 nm and 500 nm , thus disregarding scattered data and a possible purely elastic zone, and Poisson's ratio of 0.2. Thermal analysis was performed with a thermal analyzer NETZSCH STA 449 F3 Jupiter between $35 \text{ }^\circ\text{C}$ and $1100 \text{ }^\circ\text{C}$ at $10 \text{ }^\circ\text{C}/\text{min}$ under Argon atmosphere.

3. Results and Discussion

3.1. The homogeneity

The homogeneity of the samples was checked by means of Energy-Dispersive X-Ray Spectroscopy. The samples were observed with Scanning Electron Microscopy (SEM), and areas of each sample were chosen and analysed using EDS. Different points of each area were analysed, in order to certify the reliability of the results. Elemental maps with the distribution of the elements in samples $90\text{GeO}_2\cdot 10\text{K}_2\text{O}$ and $70\text{GeO}_2\cdot 10\text{K}_2\text{O}\cdot 20\text{Ta}_2\text{O}_5$ are shown in Figures 1 and 2, respectively. The distribution of the elements is quite homogeneous, except for some regions richer in Ta for the composition $70\text{GeO}_2\cdot 10\text{K}_2\text{O}\cdot 20\text{Ta}_2\text{O}_5$.

3.2. Hardness and elastic modulus of the glass samples

Figures 3 and 4 exhibit hardness and elastic modulus versus penetration depth curves, respectively, which were obtained for a test of five glass samples. The average values obtained for all the hardness tests ranged between $5.10 \pm 0.32 \text{ GPa}$ and $6.91 \pm 0.09 \text{ GPa}$.

Initially, both curves increased to a maximum value which is followed by a decrease to a constant value. Usually, the initial sharp increase in hardness at a small penetration depth is associated with the transition from purely elastic to elastic-plastic contact. The mean contact pressure just expresses the

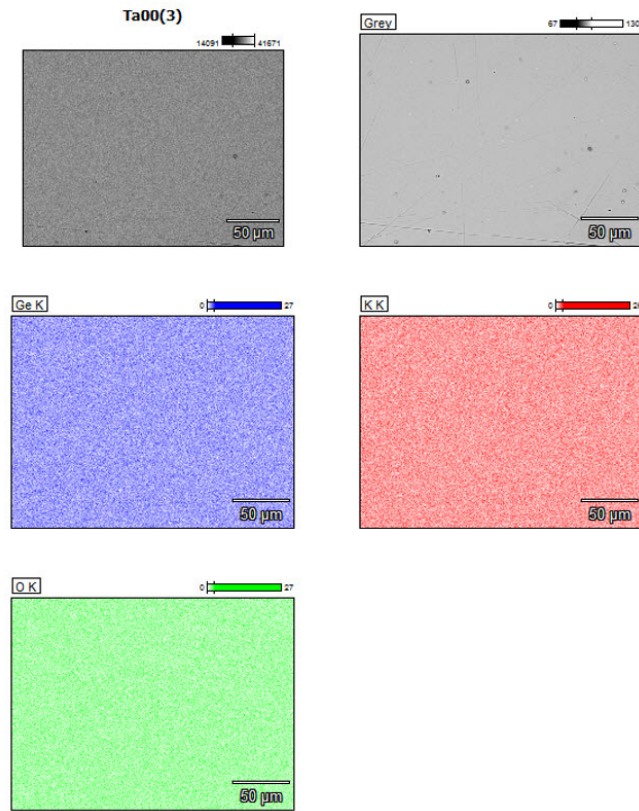


Figure 1. Elemental map of the glass sample $90\text{GeO}_2 \cdot 10\text{K}_2\text{O}$.

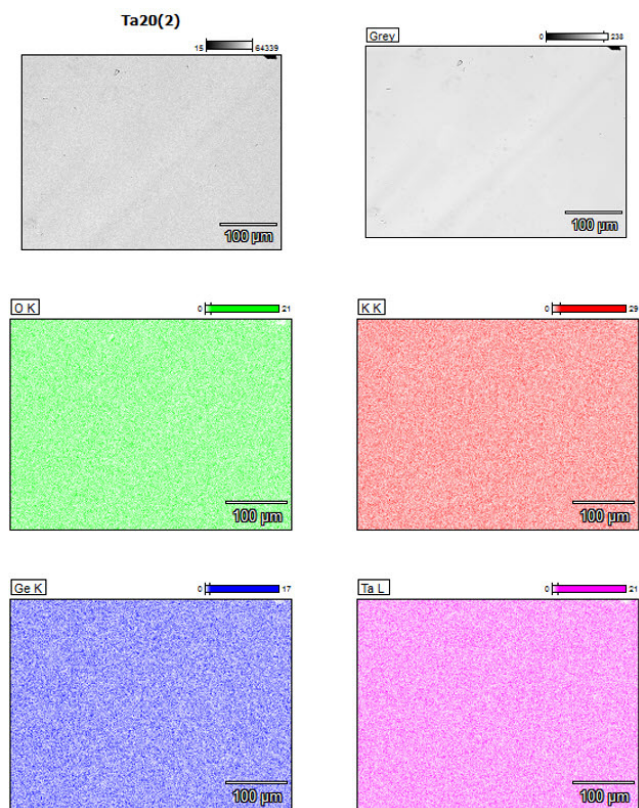


Figure 2. Elemental map of the glass sample $70\text{GeO}_2 \cdot 10\text{K}_2\text{O} \cdot 20\text{Ta}_2\text{O}_5$.

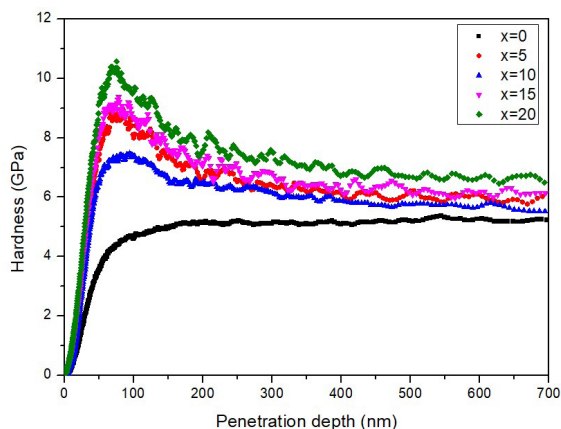


Figure 3. Hardness versus penetration depth curve for the ternary system $(90-x)\text{GeO}_2 \cdot 10\text{K}_2\text{O} \cdot (x)\text{Ta}_2\text{O}_5$.

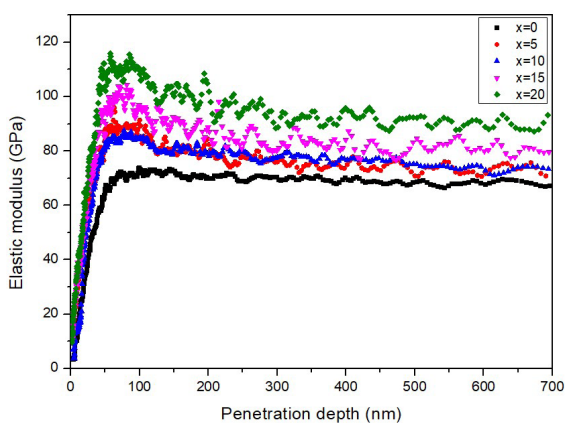


Figure 4. Elastic modulus versus penetration depth curve for the ternary system $(90-x)\text{GeO}_2 \cdot 10\text{K}_2\text{O} \cdot (x)\text{Ta}_2\text{O}_5$.

hardness under a completely developed plastic zone. Under a partially formed plastic zone or even with no plastic zone, the contact pressure is generally smaller than the nominal hardness¹⁹. Figure 3 shows that this effect is observed for all the samples containing Ta_2O_5 . Although, it is not identified for the tantalum-free composition $90\text{GeO}_2 \cdot 10\text{K}_2\text{O}$. For the samples containing Ta_2O_5 , this could be explained by the fact that in a low depth the tip is very blunt to penetrate the glass, overestimating the hardness²⁰. However, for the sample $90\text{GeO}_2 \cdot 10\text{K}_2\text{O}$, it seems that the tip starts to penetrate the glass since the beginning of the measurement due to the absence of a peak at the hardness axis.

Regarding the elastic modulus, the penetration depth dependence on the Ta_2O_5 followed the same trend observed for the hardness. Table 2 lists the average values of both properties, obtained from the measurements. The average elastic modulus measured for the five samples ranged from 69.2 ± 1.5 GPa to 92.3 ± 1.0 GPa. A pure germanate glass has a reported elastic modulus of 43.3 GPa¹⁸. The binary composition $90\text{GeO}_2 \cdot 10\text{K}_2\text{O}$ has a reported longitudinal elastic modulus of about 67 GPa²¹. In this work, a Poisson's ratio of 0.2 was used for the calculations. This value was

Table 2. Values of hardness and elastic modulus for the system $(90-x)\text{GeO}_2 \cdot 10\text{K}_2\text{O} \cdot (x)\text{Ta}_2\text{O}_5$, with x varying from 0 to 20% mol.

Composition	E (GPa)	H (GPa)
$90\text{GeO}_2 \cdot 10\text{K}_2\text{O}$	69.2 ± 1.5	5.10 ± 0.32
$85\text{GeO}_2 \cdot 10\text{K}_2\text{O} \cdot 5\text{Ta}_2\text{O}_5$	74.9 ± 1.3	6.18 ± 0.22
$80\text{GeO}_2 \cdot 10\text{K}_2\text{O} \cdot 10\text{Ta}_2\text{O}_5$	77.3 ± 7.5	5.52 ± 1.11
$75\text{GeO}_2 \cdot 10\text{K}_2\text{O} \cdot 15\text{Ta}_2\text{O}_5$	82.2 ± 0.6	6.39 ± 0.06
$70\text{GeO}_2 \cdot 10\text{K}_2\text{O} \cdot 20\text{Ta}_2\text{O}_5$	92.3 ± 1.0	6.91 ± 0.09

based on the Poisson's ratio of a pure germanate glass, which is 0.19¹⁸. The data were analysed following the methods proposed by Oliver and Pharr²².

The relation between the molar concentration of Ta_2O_5 (x), the elastic modulus, and the hardness, for compositions $(90-x)\text{GeO}_2 \cdot 10\text{K}_2\text{O} \cdot (x)\text{Ta}_2\text{O}_5$ is highlighted in Figure 5. It is remarkable that the elastic modulus increases with increasing tantalum content. The same trend appears for hardness, but, for this property, the lower hardness values observed for sample $80\text{GeO}_2 \cdot 10\text{K}_2\text{O} \cdot 10\text{Ta}_2\text{O}_5$ and the high standard deviation shown in the results of the nanoindentation tests performed for this sample, preclude concluding if this property always increases with an increasing molar concentration of Ta_2O_5 . Further studies with intermediary compositions should be conducted in order to clarify this point. However, previous investigations in these glass compositions already pointed out that other properties such as thermal stability against devitrification do not follow a linear trend against tantalum oxide content. Such behaviour was already related to a specific structural evolution of the glass network versus composition¹⁷.

In fact, as already described for this glass system¹⁷, the effect of tantalum addition in the potassium germanate glass network can be better understood considering two distinct composition ranges. For low Ta_2O_5 contents (≤ 10 mole%), TaO_6 octahedra are inserted inside the germanate covalent network (between GeO_4 tetrahedra) and promote cross-linking bonds due to tantalum high coordination number and a resulting higher overall connectivity. However, owing to the low Ta_2O_5 solubility in germanate compounds, higher contents beyond 10% progressively promote TaO_6 rich domains constituted of TaO_6 clusters. Such behaviour can be understood as the initial stage of an amorphous phase separation and a resulting nanoscale heterogeneous glass network constituted of tantalum germanate and tantalum oxide domains. In this composition range, these tantalum oxide rich domains act as crystallization nuclei in agreement with lower thermal stabilities determined by DSC¹⁷ and promote crystallization of a potassium tantalum perovskite phase of type $\text{K}_2\text{Ta}_8\text{O}_{21}$. Since Ta^{5+} has a large dissociation energy and a large cationic field strength, because of its small ionic radius and high valence state, such TaO_6 clusters could contribute to a high packing density of the glass¹, strengthening the bonds and enhancing the bond density.

The progressive increase of density with the addition of Ta_2O_5 content contributes to the high compactness of the glass structure. Previous studies²³ have already demonstrated that the Ta^{5+} ions entered into the heavy metal oxide glass as TaO_6 octahedral units, which strengthened the

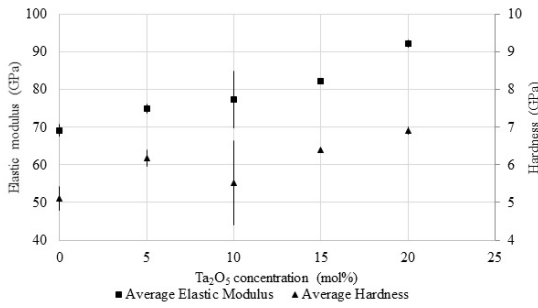


Figure 5. Relation between the molar concentration of Ta₂O₅ (x), the elastic modulus, and the hardness for compositions (90-x)GeO₂·10K₂O·(x)Ta₂O₅.

network connectivity and led to outstanding hardness. However, from a certain threshold, the further addition of Ta₂O₅ decreased the glass's mechanical stability as large nanocrystals and tantalum clusters broke the homogeneity of the glass, and when a load was applied, the cracks spread to its surrounding area.

Summarizing, an increase in the elastic modulus and hardness caused by high Ta₂O₅ contents could be explained by both factors: the intrinsic properties of the Ta₂O₅ and by the manner that the tantalum ions are inserted in the glassy structure.

3.3. The influence of crystallization on hardness and elastic modulus

As the sample 70GeO₂·10K₂O·20Ta₂O₅ exhibited the highest values of both elastic modulus and hardness, this sample was selected for investigation of its crystallization behaviour. The characteristic temperatures were obtained by thermal analysis and are labelled in Figure 6.

The first crystallization event related with potassium tantalate K₂Ta₈O₂₁ starts around 840 °C, whilst the complete crystallization is reached around 878 °C. In addition, another crystallization event is detected around 1000 °C and is attributed to crystallization of the remaining mixed potassium tantalum germanate glassy phase. A heat treatment was conducted in order to determine if the precipitation of crystalline phases could affect the mechanical properties of the glass. Therefore, the sample 70GeO₂·10K₂O·20Ta₂O₅ was heated up to the T_x, 840 °C, and kept at this temperature for 48 h. Thereafter, the sample was slowly cooled to room temperature.

The heat-treated sample was still transparent, however, showing a light bluish coloration attributed to crystals precipitation. A heat-treated 70GeO₂·10K₂O·20Ta₂O₅ sample is shown in Figure 7. In fact, light scattering due to crystallites is known to increase for lower wavelengths. The measured elastic modulus and hardness values for the heat-treated sample were 99.1 ± 2.7 GPa and 7.34 ± 0.37 GPa, such values being 7.4% and 6.2% higher than the same values obtained for the precursor glass sample.

Both pristine glass and final glass-ceramic were characterized by X-ray diffraction for a better overview of their amorphous/crystalline state and identification of precipitated crystalline phases, as shown in Figure 8. As expected, the glass sample is free of diffraction peaks

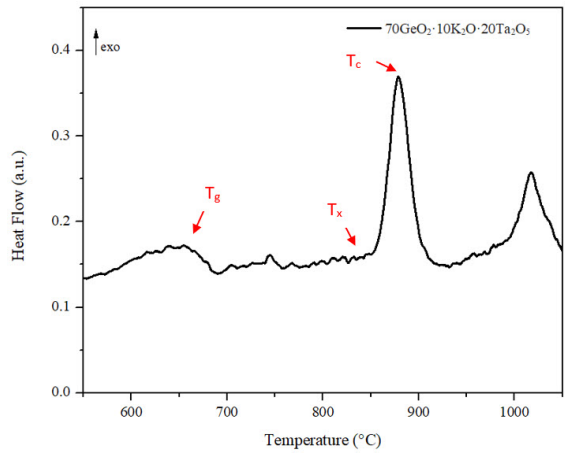


Figure 6. DSC curve of glass composition 70GeO₂·10K₂O·20Ta₂O₅.



Figure 7. Sample 70GeO₂·10K₂O·20Ta₂O₅ with a central thickness of 4.8 mm treated at 840 °C for 48 h.

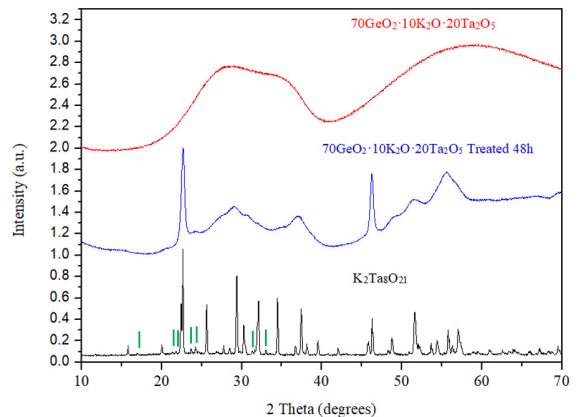


Figure 8. X-ray diffraction patterns of samples 70GeO₂·10K₂O·20Ta₂O₅, non-treated, 70GeO₂·10K₂O·20Ta₂O₅, heat-treated at 840 °C for 48 h, and K₂Ta₈O₂₁. The diffraction peaks that are in agreement with the existence of a superstructure tripling of parameter b are indicated by green symbols.

but rather exhibits diffraction halos centered around 28 and 55°, in agreement with an amorphous state. On the other hand, the heat-treated sample presents a different XRD pattern with several diffraction peaks between 10 and 70°, supporting the formation of a transparent glass-ceramic. Based on previous crystallization studies on this glass composition and by comparison with reported XRD patterns of alkaline tantalate crystalline phases, the diffraction peaks nicely match with the perovskite-type potassium tantalate $K_2Ta_8O_{21}$ as described by da Cunha et al.¹².

The crystalline structure of this perovskite is similar to tetragonal tungsten bronze $K_{0.6}WO_3$ but additional weak diffraction peaks are in agreement with the existence of a superstructure and tripling of parameter b ²⁴. In fact, the crystalline network is built from corner-shared TaO_6 octahedra in a way that free-space cavities are also formed between this octahedral framework being larger cavities labeled A_1 and A_2 of coordination 12 and 15 and smaller B cavities of coordination 9. A_1 and A_2 cavities are located one above the other along the c axis forming tunnels where large cations like potassium can be accommodated. Consequently, the increase of both elastic modulus and hardness can be mainly attributed to the corner-shared TaO_6 network similar to the structure of orthorhombic Ta_2O_5 which is known to give a large dissociation energy ($G_{Ta_2O_5} = 95.6 \text{ kJ/cm}^3$).

Based on these considerations, such tantalum oxide rich domains are suspected to be the reason for the high measured values of both elastic moduli and hardness.

Sidek et al.²⁵ reported the elastic moduli of germanate glasses containing lead and bismuth in the form of $(GeO_2)_{60} \cdot (PbO)_{40-x} \cdot (1/2Bi_2O_3)_x$ where $x = 0$ to 40 mol%. The results indicated that the elastic moduli increased linearly with Bi_2O_3 content, with Young's modulus ranging between 54.93 GPa ($x=0$) and 64.90 GPa ($x=40$). The increase in elastic moduli was attributed to an increase in the cross-link density and, therefore, an increase in the rigidity of glass samples.

Bayya et al.²⁶ demonstrated that the mechanical properties of the $20BaO \cdot 10Ga_2O_3 \cdot 70GeO_2$ (BGG) molar glass composition can be dramatically improved by forming a glass-ceramic. The results indicated that glass ceramization resulted in a 40% improvement in hardness, which was attributed to the hexagonal close-packed structure of the $BaGe_4O_9$ phase and its high atomic packing density compared with those in the parent glass. The BGG glass-ceramic has an elastic modulus of 116 GPa, which is 65% higher than that of the parent BGG glass (70 GPa). The observed increase was associated with the contribution of the crystalline phase ($BaGe_4O_9$) present in the glass-ceramic. As in the potassium tantalum germanate system, the selective precipitation promoted by controlled crystallization proved to be a tool to achieve high values of the elastic modulus and hardness while keeping the transparency of the material.

Furthermore, the same study²⁶ reported a 134% increase in the fracture toughness of the BGG glass-ceramic and a 116% increase in strength over the parent glass. Crack deflection at the grain boundary is believed to be the main factor contributing to the observed increase in fracture toughness, and the increase in strength is reported as a result of the increase in fracture toughness and elastic modulus.

Although fracture toughness and strength were not evaluated for the potassium tantalum germanate system, we encourage the investigation of these properties in future works as the precipitation of nanocrystals might help to prevent the propagation of cracks in the structure of the material. Investigation of the crystals in the heat-treated $70GeO_2 \cdot 10K_2O \cdot 20Ta_2O_5$ sample using scanning electron microscopy (SEM) is also suggested.

4. Conclusions

The introduction of tantalum oxide in germanate glasses improves their mechanical properties, resulting in samples with high elastic moduli and hardness. The elastic modulus of samples containing from 0% to 20% mol. of Ta_2O_5 , ranged between $69.2 \pm 1.5 \text{ GPa}$ and $92.3 \pm 1.0 \text{ GPa}$, while the hardness of the same samples varied between $5.10 \pm 0.32 \text{ GPa}$ and $6.91 \pm 0.09 \text{ GPa}$. This relevant improvement of mechanical properties can be related with structural changes with a progressive formation and corner-shared TaO_6 rich domains with high dissociation energies within the mixed tantalum germanate network. Selective crystallization of the perovskite type $K_2Ta_8O_{21}$ results in transparent glass-ceramics with further improved mechanical properties with an elastic modulus of $99.1 \pm 2.7 \text{ GPa}$ and a hardness of $7.34 \pm 0.37 \text{ GPa}$.

5. Acknowledgments

Ruud Hendrikx at the Department of Materials Science and Engineering of the Delft University of Technology is acknowledged for the X-ray analysis. The Brazilian National Council for Scientific and Technological Development (CNPq) is acknowledged for the granted PhD scholarship (202950/2014-0).

6. References

- Rosales-Sosa GA, Masuno A, Higo Y, Inoue H, Yanaba Y, Mizoguchi T, et al. High elastic moduli of a $54Al_2O_3 \cdot 46Ta_2O_5$ glass fabricated via containerless processing. *Sci Rep.* 2015;5:15233.
- Justino de Lima CL. Innovative low-melting glass compositions containing fly ash and blast furnace slag [thesis]. Netherlands: Delft University of Technology; 2020.
- Makishima A, Mackenzie JD. Direct calculation of Young's modulus of glass. *J Non-Cryst Solids.* 1973;13:35-45.
- Plucinski M, Zwanziger JW. Topological constraints and the Makishima-Mackenzie model. *J Non-Cryst Solids.* 2015;429:20-3.
- Yamane M, Mackenzie JD. Vickers hardness of glass. *J Non-Cryst Solids.* 1974;15:153-64.
- Poirier G, Messadeq Y, Ribeiro SJL, Poulain M. Structural study of tungstate fluorophosphate glasses by Raman and X-ray absorption spectroscopy. *J Solid State Chem.* 2005;178(5):1533-8.
- Araujo CC, Strojek W, Zhang L, Eckert H, Poirier G, Ribeiro SJL, et al. Structural studies of $NaPO_3 \cdot WO_3$ glasses by solid state NMR and Raman spectroscopy. *J Mater Chem.* 2006;16:3277-84.
- Poirier G, Cassanjes FC. Structural study of glasses in the binary system $NaPO_3 \cdot MoO_3$ by X-ray absorption spectroscopy at the Mo K and L3 edges. *Mater Chem Phys.* 2010;120(2-3):501-4.
- de Lima CLJ, Pastena B, Nardi RPRD, Gouvêa JT Jr, Ferrari JL, Cassanjes FC, et al. Thermal, structural and crystallization study of niobium potassium phosphate glasses. *Mater Res.* 2015;18(2):13-6.

10. Cordeiro L, Silva RM, de Pietro GM, Pereira C, Ferreira EA, Ribeiro SJL, et al. Thermal and structural properties of tantalum alkali-phosphate glasses. *J Non-Cryst Solids*. 2014;402:44-8.
11. Cunha CR, Maestri SA, Sousa BP, Marcondes LM, Gonçalves RR, Cassanjes FC, et al. Alkali metal tantalum germanate glasses and glass-ceramics formation. *J Non-Cryst Solids*. 2018;499:401-7.
12. Cunha CR, Marcondes LM, Batista G, Gonçalves RR, Cassanjes FC, Poirier GY. Crystallization of bronze-like perovskite in potassium tantalum germanate glasses: glass ceramic preparation and its optical properties. *Opt Mater*. 2021;122(Part B):111803.
13. Marcondes LM, da Cunha CR, de Pietro GM, Manzani D, Gonçalves RR, Batista G, et al. Multicolor tunable and NIR broadband emission from rare-earth-codoped tantalum germanate glasses and nanostructured glass-ceramics. *J Lumin*. 2021;239:118357.
14. Inaba S, Fujino S, Morinaga K. Young's modulus and compositional parameters of oxide glasses. *J Am Ceram Soc*. 1999;82:3501-7.
15. Rosales-Sosa GA, Masuno A, Higo Y, Inoue H. Crack-resistant Al_2O_3 - SiO_2 glasses. *Sci Rep*. 2016;6:23620.
16. Meng D, Yi J, Zhao DQ, Ding DW, Bai HY, Pan MX, et al. Tantalum based bulk metallic glasses. *J Non-Cryst Solids*. 2011;357(7):1787-90.
17. De Pietro GM, Pereira C, Gonçalves RR, Ribeiro SJL, Freschi CD, Cassanjes FC, et al. Thermal, structural, and crystallization properties of new tantalum alkali-germanate glasses. *J Am Ceram Soc*. 2015;98:2086-93.
18. Rouxel T. Elastic properties and short-to medium-range order in glasses. *J Am Ceram Soc*. 2007;90:3019-39.
19. Jian SR, Chang HW, Tseng YC, Chen PH, Juang JY. Structural and nanomechanical properties of BiFeO_3 thin films deposited by radio frequency magnetron sputtering. *Nanoscale Res Lett*. 2013;8(1):297.
20. Tadjiev DR, Hand RJ. Inter-relationships between composition and near surface mechanical properties of silicate glasses. *J Non-Cryst Solids*. 2008;354:5108-9.
21. Mamiya S, Matsude Y, Kaneda K, Kawashima M, Kojima S. Brillouin scattering study of binary potassium germanate glasses. *Mater Sci Eng B*. 2010;173(1-3):155-7.
22. Oliver WC, Pharr G. An improved technique for determining hardness and elastic modulus using load and displacement sensing indentation experiments. *J Mater Res*. 1992;7:1564-83.
23. Zhang X, Chen Q, Zhang S. Ta_2O_5 nanocrystals strengthened mechanical, magnetic, and radiation shielding properties of heavy metal oxide glass. *Molecules*. 2021;26(15):4494.
24. Chaminade JP, Pouchard M, Hagenmuller P. Tantalates and oxyfluorotantalates of sodium. *Rev. Chem. Min*. 1972;9:381.
25. Sidek HAA, Bahari HR, Halimah MK, Yunus WMM. Preparation and elastic moduli of germanate glass containing lead and bismuth. *Int J Mol Sci*. 2012;13(4):4632-41.
26. Bayya SS, Sanghera JS, Aggarwal ID, Wojcik JA. Infrared transparent germanate glass-ceramics. *J Am Ceram Soc*. 2002;85:3114-6.